



## Radiolytic syntheses of nanoparticles in supramolecular assemblies

Qingde Chen, Xinghai Shen<sup>\*</sup>, Hongcheng Gao

Beijing National Laboratory for Molecular Sciences, Radiochemistry and Radiation Chemistry Key Laboratory of Fundamental Science, College of Chemistry and Molecular Engineering, Peking University, Beijing 100871, PR China

### ARTICLE INFO

Available online 13 May 2010

#### Keywords:

Ionizing radiation  
Nanoparticles  
Supramolecular assembly  
Microemulsion(s)  
Ionic liquid(s)  
Cyclodextrin(s)  
Hydrated electron

### ABSTRACT

Ionizing radiation is a powerful method in the syntheses of nanoparticles (NPs). The application of ionizing radiation in supramolecular assemblies can afford us more unique conditions to control the composition and morphology of the NPs. So far, most work focused on water-in-oil (W/O) microemulsions or reversed micelles. In this supramolecular organization, it has been proved that the effects of many conditions on the yield of  $e_{aq}^-$  play a key role, remarkably different from the mechanism in routine chemical method. Besides, some supramolecular assemblies of cyclodextrins and ionic liquids have been used in the syntheses of NPs by ionizing radiation, and many novel and interesting phenomena appeared. This review is intended to underline the three significant aspects of the radiolytic syntheses of NPs in supramolecular assemblies.

© 2010 Elsevier B.V. All rights reserved.

### Contents

1. Introduction . . . . .	32
2. Radiolytic syntheses of nanoparticles in water-in-oil microemulsions . . . . .	33
2.1. Principle of radiolytic syntheses of nanoparticles in solutions . . . . .	33
2.2. Principle of syntheses of nanoparticles in microemulsions by routine chemical method . . . . .	33
2.3. Composition and morphology control of nanoparticles depending on the structural change of microemulsions and absorbed dose in irradiation method . . . . .	34
2.4. Composition and morphology control of nanoparticles by the yield of hydrated electrons in microemulsions . . . . .	35
2.4.1. Controlled reduction of $Cu^{2+}$ in microemulsions . . . . .	36
2.4.2. Radiolytic syntheses of octahedral $Cu_2O$ nanocrystals . . . . .	37
2.4.3. Radiolytic syntheses of solid and hollow $Cu_2O$ nanocubes . . . . .	38
2.5. Research on the growth kinetics of nanoparticles in microemulsion by ionizing radiation . . . . .	39
3. Radiolytic syntheses of nanoparticles in other supramolecular assemblies . . . . .	40
3.1. Radiolytic syntheses of nanoparticles controlled by cyclodextrins . . . . .	40
3.2. Radiolytic syntheses of nanoparticles in ionic liquids . . . . .	41
4. Conclusions and prospects . . . . .	42
Acknowledgments . . . . .	43
References . . . . .	43

### 1. Introduction

In the realm of nanoscience and nanotechnology, the largest activity has been focused on the syntheses of new nanoparticles (NPs) with different sizes and shapes, which have strong effects on their widely varying properties and applications [1–6]. To realize the size and shape control of NPs, a variety of methods have been employed. Meanwhile,

supramolecular assemblies (such as microemulsions, liquid crystals, vesicles, and so on) are powerful templates for preparing NPs [1,7–18], which are polymolecular entities that result from the spontaneous association of a large undefined number of components into a specific phase having more or less well-defined microscopic organization and macroscopic characteristics depending on its nature [19]. As for the radiolytic syntheses of NPs concerning supramolecular assemblies, most work is focused on water-in-oil (W/O) microemulsions or reversed micelles. W/O microemulsions, consisting of surfactant, oil, water as well as cosurfactant in most cases, can provide us with particularly attractive microreactors for preparing NPs, whose morphology can be

<sup>\*</sup> Corresponding author. Tel.: +86 10 62765915; fax: +86 10 62759191.  
E-mail address: [xshen@pku.edu.cn](mailto:xshen@pku.edu.cn) (X. Shen).

well controlled [1,7,9–13]. Now, the combination of ionizing radiation and W/O microemulsion has become a novel and important way in the synthesis of NPs, and has attracted much attention. Especially, it was found that this method can afford us more unique conditions to control the composition, morphology and size of NPs. Furthermore, it was confirmed that the effects of these conditions on the yield of  $e_{aq}^-$  play a key role, remarkably different from the mechanism in routine chemical method. Besides, ionizing radiation is also important in the research on the growth kinetics of NPs. However, there is no review article published so far.

Besides W/O microemulsions, other supramolecular assemblies began to attract attention in the radiolytic syntheses of NPs. Cyclodextrins (CDs), a series of cyclic oligomers consisting of six or more  $\alpha$ -1,4-linked D-glucopyranose units, are the most important hosts in supramolecular chemistry. They can form plentiful assemblies (e.g., aggregates of CDs, aggregates of CD inclusion complexes, cyclodextrin rotaxanes and polyrotaxanes, cyclodextrin nanotubes and their secondary assembly) [20,21]. Ionic liquids (ILs), a kind of organic salt, are liquids at or near room temperature. Now, they are regarded as an attractive class of green solvents in the syntheses of nanoparticles and nanostructures because of their novel and tunable physical–chemical properties [22–24]. In ILs, there also exist three-dimensional supramolecular networks with polar and non-polar regions [25–27]. These supramolecular assemblies of CDs and ILs have been used in the syntheses of NPs by ionizing radiation, and many novel and interesting phenomena appeared, which are also worthwhile to be reviewed.

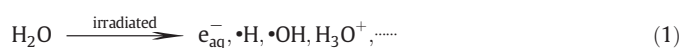
Therefore, in the present article, the above three significant aspects on the radiolytic syntheses of NPs in supramolecular assemblies will be included.

## 2. Radiolytic syntheses of nanoparticles in water-in-oil microemulsions

The radiolytic syntheses of NPs in W/O microemulsions combined the characters of the syntheses of NPs in solutions by ionizing radiation and in W/O microemulsion by routine chemical method, and appeared many novel properties. For comparison, firstly, the principle and characters of the syntheses of NPs by the two methods are simply described, respectively.

### 2.1. Principle of radiolytic syntheses of nanoparticles in solutions

Among the numerous methods of preparing NPs, ionizing radiation (such as  $\gamma$ -irradiation, electron beam irradiation and so on) is powerful, since it can conveniently produce a series of species with tunable redox potentials, not be achievable by other means, in a wide range of temperature [28–31]. For example, in aqueous solution, the water molecules absorb the irradiation energy and generate many reactive species, such as hydrated electrons ( $e_{aq}^-$ ),  $\bullet H$  and  $\bullet OH$  (Eq. (1)) [32].



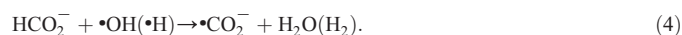
The reducing species, i.e.,  $e_{aq}^-$  and  $\bullet H$ , reduce the precursors in aqueous solution, leading to the formation of NPs via a series of coalescence processes. Because the oxidizing radicals (such as  $\bullet OH$ ) can react with reducing species (see Eq. (2) [32]) and oxidate the reduction product, it should be eliminated by some additives (such as alcohols, formates) (Eqs. (3) and (4) [32]). Different additives will generate a series of reducing radicals with tunable redox potentials (Table 1) [33], which can reduce the precursors selectively.



**Table 1**  
Standard redox potentials of some radiation-generated species.<sup>a</sup>

Species	$e_{aq}^-$	$\bullet CO_2^-$	$(CH_3)_2\dot{C}OH$	$CH_3\dot{C}OH$	$\bullet CH_2OH$	$\bullet OH$
$E^0/V$	−2.9	−1.9	−1.5	−1.1	−0.9	1.9

<sup>a</sup> Taken from Ref. [33].



In organic solvents, similar reactions and processes take place, too. As a typical example, the detail formation process of metal clusters and NPs in solution by ionizing radiation is illustrated in Fig. 1.

In general, dose rate and additives (such as ligand, surfactant, etc.) are always used to control the size, shape and structure of the obtained NPs. So far, besides few report about metal halide and nonmetal NPs [34–37], great efforts have been focused on the syntheses of metal, core–shell metal or alloy, and metal chalcogenide NPs in aqueous solution and organic solvent, which have been well reviewed in the reference [28–31,38,39]. Recently, for the first time, we obtained BaSO<sub>4</sub> NPs by precipitating Ba<sup>2+</sup> ions with SO<sub>4</sub><sup>2−</sup> ions, which were generated via the radiolytic reduction of S<sub>2</sub>O<sub>8</sub><sup>2−</sup> (Eq. (5)) [40]. This extends the application of ionizing radiation in nanoscience and nanotechnology.



### 2.2. Principle of syntheses of nanoparticles in microemulsions by routine chemical method

In the syntheses of NPs in microemulsions by routine chemical method, a two-microemulsion method is most popular [10,11]. In the method, two microemulsions, containing one corresponding reagent, are mixed (Fig. 2A). Thereafter, the water pools collide, coalesce to form transient water pool dimers, exchange the water contents, and disintegrate into new water pools, continuously. Then, the reaction takes place inside the water pools, which is followed by nucleation, growth, ripening, and coagulation of primary particles, resulting in the formation of the final NPs surrounded by water and/or stabilized by surfactants. In addition, a single-microemulsion method that includes a number of variations has also been frequently used for the nanoparticle synthesis in microemulsion [10,11]. In this approach, one of the reactants can be added directly, in the form of a solution or a solid, liquid, or gas, to the microemulsion carrying the other reactant (Fig. 2B).

Because the reaction takes place in the water pool or on the interface of water and oil, the nucleation and growth processes of NPs are affected by the size and shape of water pool, the rigidity of the interface, the concentration of reactant, and so forth. Moreover, the size and shape of water pool, and the rigidity of the interface could be controlled by  $\omega$  value (molar ratio of water to surfactant), additives (such as short-chain alcohols, salts), etc. Thus, the size and morphology of NPs could be well adjusted [41–47]. For example, the presence of short-chain alcohols and benzyl alcohols can reduce the rigidity of a microemulsion, and increase the exchange rate of water pool, resulting in the formation of the bigger NPs with a wider size distribution [41,42]. Bagwe and Khilar [41] found that there is a weak effect of cations on the average size of the synthesized AgCl NPs in AOT-based microemulsions. However, the use of hydrolyzable monovalent cations (such as Li<sup>+</sup> and Na<sup>+</sup>) can lead to a higher exchange coefficient, which is propitious to the formation of AgCl NPs [41]. In addition, the preferential adsorption of surfactant or counter ions on some crystal faces of NPs could be used to control the aggregation or growth of NPs, and the resulting morphology [48–51]. Filankembo et al. [51] found that Cl<sup>−</sup> favors the generation of Cu nanorods with higher aspect ratio in a Cu(AOT)<sub>2</sub>-isooctane–water

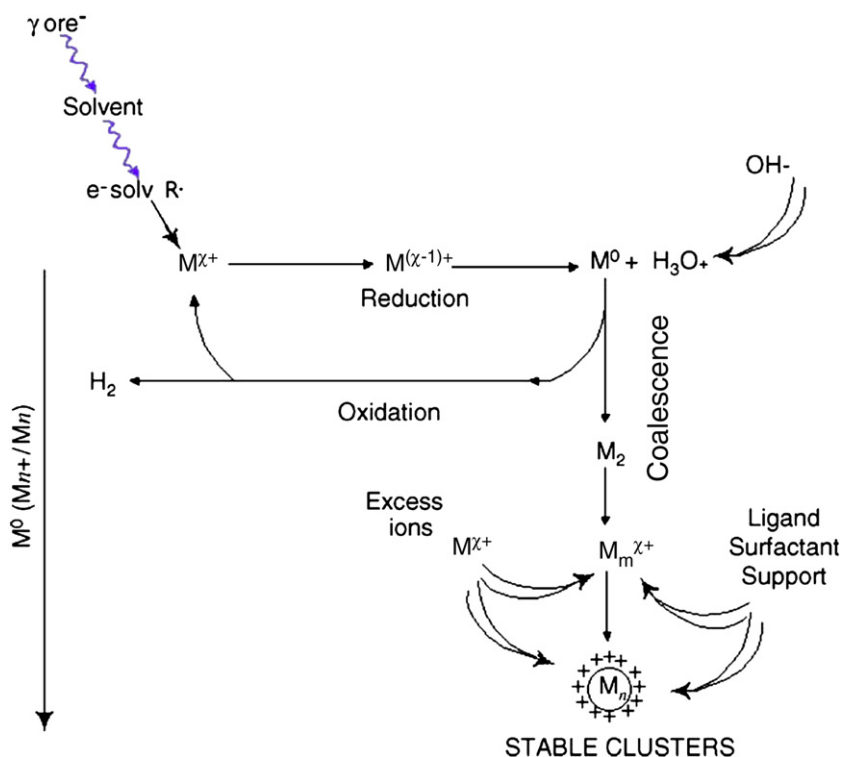


**Fig. 1.** Scheme of the reduction of metal ion in solution by ionizing radiation. Additive (such as alcohol) is added in order to scavenge oxidizing radicals (such as  $\cdot\text{OH}$ ). The isolated atoms formed  $\text{M}^0$  coalesce into clusters. They absorb excess ions. They are stabilized by ligands, polymers or supports. The redox potential  $E^0(\text{M}_n^{x+}/\text{M}_n)$  increases with the nuclearity. The smallest oligomers may undergo reverse corrosion. Taken from Ref. [31].

system, where hydrazine was used as a reducing agent. This phenomenon was ascribed to the preferential adsorption of  $\text{Cl}^-$  on the {001} faces and the faster growth on the {111} faces of Cu nanocrystals (NCs). However,  $\text{NO}_3^-$  did not exhibit a similar action.

### 2.3. Composition and morphology control of nanoparticles depending on the structural change of microemulsions and absorbed dose in irradiation method

Different from routine chemical method, the generation of reducing species in microemulsion is *in situ*. Thus, the combination of ionizing radiation and W/O microemulsion is an effective way in the synthesis of NPs. So far, Au [52], Ag [53–56], Cd–Ag Alloy [56], Cd [57], Pd [57], Cu [57], Zn [58], Ni [59], CdS [60–62], ZnS [60], PbS [63] and  $\text{Fe}_{3-x}\text{O}_4$  [64,65] NPs have been synthesized by this means in different research groups, which are summarised in Table 2. However, most of the synthesized NPs are spherical [53,56,57,59,60,62–65]. Meanwhile, a few documents reported how to control the size [53,56,60] and shape [61] of the obtained NPs.

In a sodium dodecyl sulfate (SDS)-based microemulsion, Kapoor et al. [56] accommodated  $\omega$  value to control the size of Ag NPs by electron beam irradiation. Zhang et al. [53] synthesized Ag NPs in a sodium bis-(2-ethylhexyl)sulfosuccinate (AOT)-based microemulsion by  $\gamma$ -irradiation. They found that the addition of sodium dodecyl benzene sulfonate (SDBS) could significantly lower the AOT proportion and make the Ag NPs larger [53]. Furthermore, they transferred the radiolytic reduction of  $\text{S}_2\text{O}_3^{2-}$  (Eq. (6)) and the formation of metal sulfide NPs from aqueous solution to microemulsions, and synthesized CdS and ZnS NPs in a SDS-based microemulsion, whose size was controlled *via* adjusting the ratio of water to oil [60].



Later, they added hydroxyethyl cellulose (HEC) into the microemulsion, where octylphenyl poly(ethylene glycol) ether ( $n=4$ ) (OP-4)

and octylphenyl poly(ethylene glycol) ether ( $n=10$ ) (OP-10) were used as surfactant, and transformed the morphology of CdS NPs from sphere to nanorod [61]. Moreover, the length and diameter of the CdS nanorod reduced with the decrease of  $\omega$  value [61].

In the radiolytic syntheses of NPs, the precursors also affected the reduction products. In a SDS-microemulsion, when the absorbed dose was 16 kGy and the concentration of  $\text{Cu}^{2+}$  in water pool was  $1 \times 10^{-3} \text{ mol L}^{-1}$ , the reduction product of CuCl was Cu NPs, while that of  $\text{CuSO}_4$  was a complex of  $\text{Cu}^+$  with SDS [57]. Kapoor et al. [57] considered that the reaction between  $\text{Cu}^{2+}$  and  $e_{\text{aq}}^-$  (Eq. (7)), rather than that between  $\text{Cu}^+$  and  $e_{\text{aq}}^-$  (Eq. (8)), takes place under such conditions and the generated  $\text{Cu}^+$  is stabilized by SDS when  $\text{CuSO}_4$  is used as precursor. While CuCl is used, there is no competitive reaction with reaction (8), which favors the generation of Cu NPs.



Different from the syntheses of NPs in aqueous solutions, in microemulsions, the precursors insoluble in aqueous solution can be used, which make the selection of the precursors more plentiful. In an OP-4 and OP-10-based microemulsion, PbS quantum dots were obtained by the reactions between  $\text{Pb}^{2+}$  ions with  $\text{S}^{2-}$  ions, which were generated *via* the reduction of  $\text{CS}_2$  by  $e_{\text{aq}}^-$  (Eqs. (9) and (10)) [63].



Zhang et al. [63] suggested that the reducing reaction take place at the oil–water interface (Fig. 3). In a SDS-based microemulsion,  $\text{Pd}_3[\text{SSP}(\text{OC}_2\text{H}_5)_2](\text{Ph}_3\text{P})_2\text{S}_2$ , insoluble in water, was used as precursor to synthesize Pd NPs by ionizing radiation [57]. Kapoor et al. [57]

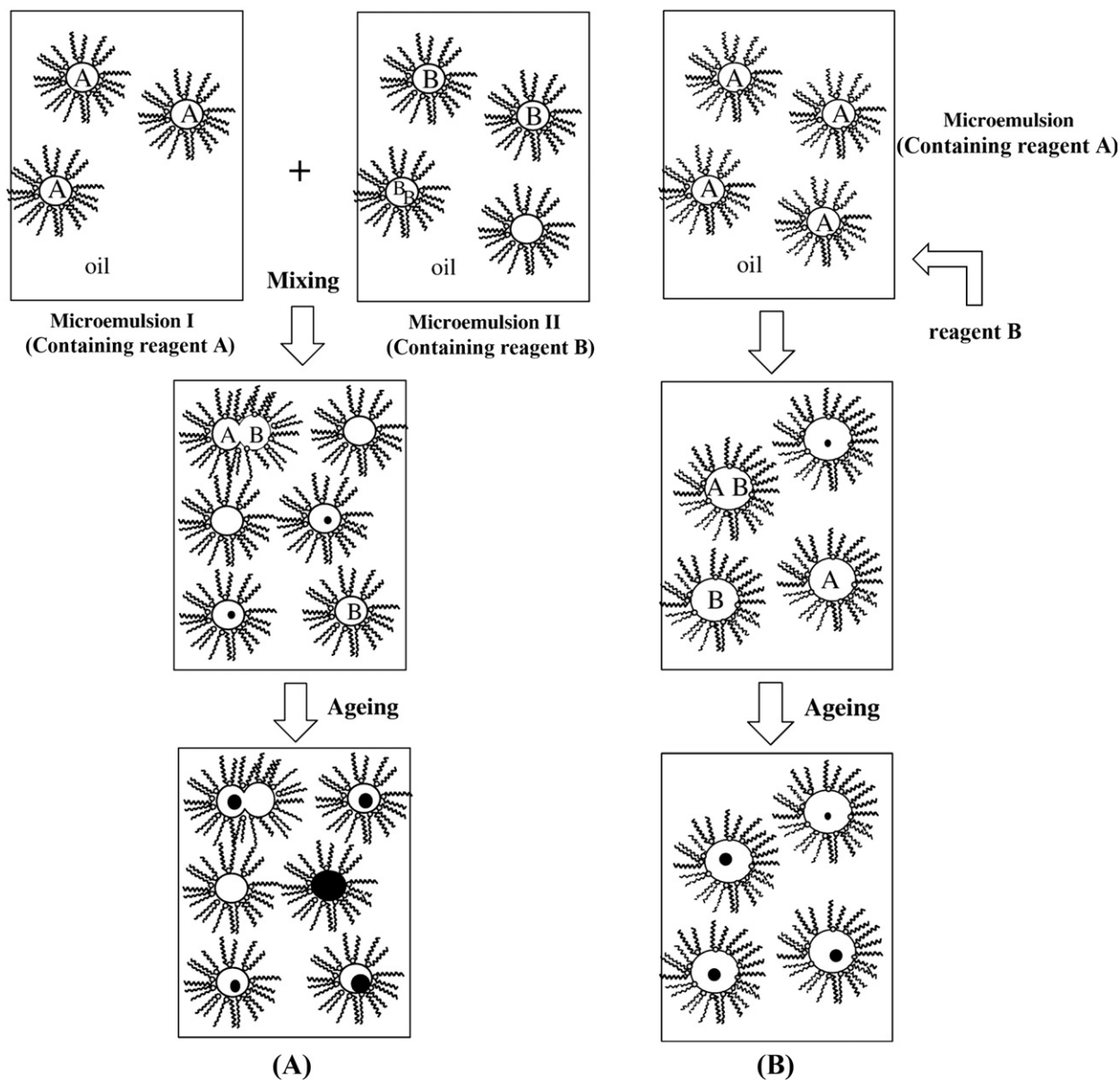


Fig. 2. Schematic illustration of the synthesis of NPs in microemulsions by routine chemical method. Taken from Ref. [11].

considered that the Pd precursor was reduced by the  $e_{aq}^-$  diffused in the oil phase.

In the radiolytic preparation of NPs, the precursors can not only be soluble in water pool, oil–water interface or oil phase, but also be pre-existing NPs. In a Triton X-100-based microemulsion, Gotic et al. [64] obtained goethite NPs by routine chemical method, which were about 200–300 nm long and up to 10 nm wide. Through  $\gamma$ -irradiation under  $N_2$  atmosphere, the goethite particles were transformed to substoichiometric magnetite ( $Fe_{3-x}O_4$ ) NPs, with the diameter ranging from 5 to 20 nm, at an absorbed dose of 460 kGy in the microemulsion [64]. Later, they further found that the  $x$  value decreased with the increase of absorbed dose [65].

Indeed, it has been found that the combination of ionizing radiation and microemulsion can afford us more unique conditions to control the composition, morphology and size of NPs.

#### 2.4. Composition and morphology control of nanoparticles by the yield of hydrated electrons in microemulsions

In the preparation of NPs in microemulsion by irradiation method, most of the work always considered that  $e_{aq}^-$  comes from the radiolysis

of water in the water pool, which is similar to the situation in the radiolytic syntheses of NPs in aqueous solution. Indeed, according to the results of pulse radiolytic investigation on the microemulsion system, when a microemulsion is irradiated,  $e_{aq}^-$  can be mainly generated from the scavenging of excess electrons, which are produced originally through the radiolysis of oil, by water pool (Fig. 4) [66–72]. Although the radiolysis of water in the water pool can also generate  $e_{aq}^-$  directly (Fig. 4 and Eq. (1)), it is less important [66–72]. In the radiolytic syntheses of Ag, Cd, Pd and Cu NPs in SDS-based microemulsion, Kapoor et al. [55–57] have ever mentioned the dual resources of  $e_{aq}^-$ . Gotic et al. [65] also noticed the existence of this regularity in the synthesis of  $Fe_{3-x}O_4$  NPs by  $\gamma$ -irradiation in the Triton X-100-based microemulsion. How to control the composition and morphology of NPs by this regularity? Before our systematic work, it is not clear.

Besides, in microemulsions, the yield of  $e_{aq}^-$  always less than 2 [68,69], is very much lower than that in pure water, which is known to be 2.7. As the increase of  $\omega$  value, the yield of  $e_{aq}^-$  usually increases [66–69,71,72], and the rate constant of the reaction between  $e_{aq}^-$  and many metal ions (e.g.,  $Ag^+$ ,  $Tl^+$ ,  $Co^{2+}$ ,  $Ni^{2+}$ ,  $Cd^{2+}$  and  $Cu^{2+}$ ) increases [55–57]. Nevertheless, these rate constants are all much lower than



**Table 2**  
Summary of the radiation-synthesized NPs in microemulsion by other research groups.

	Shape	Precursor	Surfactant	Cosurfactant	Oil phase	Factors affecting the size or shape	Type of irradiation	Refs.
Au		HAuCl <sub>4</sub>	PEGDE		<i>n</i> -Hexane		EB	[52]
Ag	Spherical	AgNO <sub>3</sub>	AOT; AOT + SDBS		Kerosene		γ-Ray	[53]
		AgNO <sub>3</sub>	AOT		Isooctane		γ-ray	[54]
Cd–Ag Alloy	Spherical	AgClO <sub>4</sub>	SDS	1-Pentanol	Cyclohexane	ω value	EB	[55]
		AgClO <sub>4</sub>	SDS	1-Pentanol	Cyclohexane		EB	[56]
Cd	Spherical	CdSO <sub>4</sub> + AgClO <sub>4</sub>	SDS	1-Pentanol	Cyclohexane		EB	[57]
Pd	Spherical	Pd <sub>3</sub> [SSP(OC <sub>2</sub> H <sub>5</sub> ) <sub>2</sub> ](Ph <sub>3</sub> P) <sub>2</sub> S <sub>2</sub>	SDS	1-Pentanol	Cyclohexane		EB; γ-ray	[57]
Zn		Zn(HCOO) <sub>2</sub>	AOT		Isooctane		γ-ray	[58]
Ni	Spherical	Ni(NO <sub>3</sub> ) <sub>2</sub>	AOT		Isooctane		γ-ray	[59]
Cu		CuCl	SDS	1-Pentanol	Cyclohexane		EB	[57]
CdS	Nanorod	CdSO <sub>4</sub> + Na <sub>2</sub> S <sub>2</sub> O <sub>3</sub>	OP-10 + OP-4		Cyclohexane	HEC as additive; ω value	γ-ray	[61]
	Spherical	Cd <sup>2+</sup> + Na <sub>2</sub> S <sub>2</sub> O <sub>3</sub>	OP-10 + OP-4		Kerosene	ratio of water to oil	γ-ray	[60]
	Spherical	CdCl <sub>2</sub> + thioacetamide	OP-10 + OP-4		Cyclohexane		γ-ray	[62]
ZnS	Spherical	Zn <sup>2+</sup> + Na <sub>2</sub> S <sub>2</sub> O <sub>3</sub>	OP-10 + OP-4		Kerosene	ratio of water to oil	γ-ray	[60]
PbS	Spherical	Pb(CH <sub>3</sub> COO) <sub>2</sub> + CS <sub>2</sub>	OP-10 + OP-4		Kerosene		γ-ray	[63]
Fe <sub>3-x</sub> O <sub>4</sub>	Spherical	FeCl <sub>3</sub> + FeSO <sub>4</sub> + OH <sup>-</sup>	Triton X-100	1-Pentanol	Cyclohexane		γ-ray	[64]
	Spherical	FeCl <sub>3</sub> + OH <sup>-</sup>	Triton X-100	1-pentanol	Cyclohexane		γ-ray	[65]

PEGDE, pentaethylene glycol dodecyl ether; EB, electron beam; AOT, sodium bis-(2-ethylhexyl)sulfosuccinate; SDBS, sodium dodecyl benzene sulfonate; SDS, sodium dodecyl sulfate; OP-10, octylphenyl poly(ethylene glycol) ether (*n* = 10); OP-4, octylphenyl poly(ethylene glycol) ether (*n* = 4); HEC, hydroxyethyl cellulose; Triton X-100, (CH<sub>3</sub>)<sub>3</sub>CCH<sub>2</sub>C-(CH<sub>3</sub>)<sub>2</sub>C<sub>6</sub>H<sub>4</sub>(OCH<sub>2</sub>CH<sub>2</sub>)<sub>n</sub>OH (*n* = 9–10).

those in aqueous solution, respectively [55–57]. In cationic-surfactant-based microemulsions, the yield of  $e_{aq}^-$  remains almost constant at 0.9, which is almost one-third of the value in bulk water [70]. Fendler group [73] reported that in the AOT-based microemulsion, the reactivity of  $e_{aq}^-$  could be reduced by an increase in the viscosity of the water pool. These regularities should be useful in the composition and morphology control of NPs by irradiation method.

Therefore, the condition for controlling the syntheses of NPs should be plentiful. If adding some electron scavengers (such as aromatic compounds in oil phase, NO<sub>3</sub><sup>-</sup> in water pool and the (co)-surfactant containing aromatic rings at interface) or adjusting the ω value, the yield of  $e_{aq}^-$  will be well accommodated, which is further used to control the composition and morphology of the synthesized

NPs by ionizing radiation. This idea for controlling the yield of  $e_{aq}^-$  is well illustrated in Fig. 4. Contrasting to the routine chemical methods, the application of radiation technology on microemulsions is characteristic, the picture of the mechanism is clear, and affords us more unique conditions to control the composition and morphology of NPs.

#### 2.4.1. Controlled reduction of Cu<sup>2+</sup> in microemulsions

In nonionic surfactants (Brij 30, Brij 56 and Triton X-100) based microemulsions, the ω value, the counterions of Cu<sup>2+</sup> and surfactant can remarkably affect the reduction of Cu<sup>2+</sup> by γ-irradiation (Table 3) [74]. It was proved that the effects of these conditions on the yield of

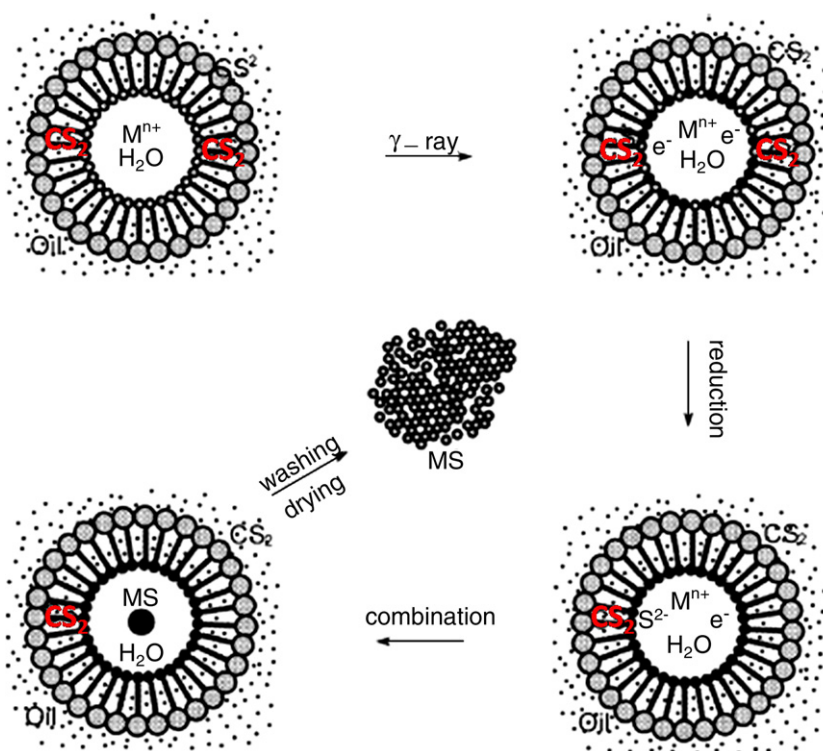


**Fig. 3.** The role of microemulsion on the formation of spherical PbS quantum dots. Taken from Ref. [63].

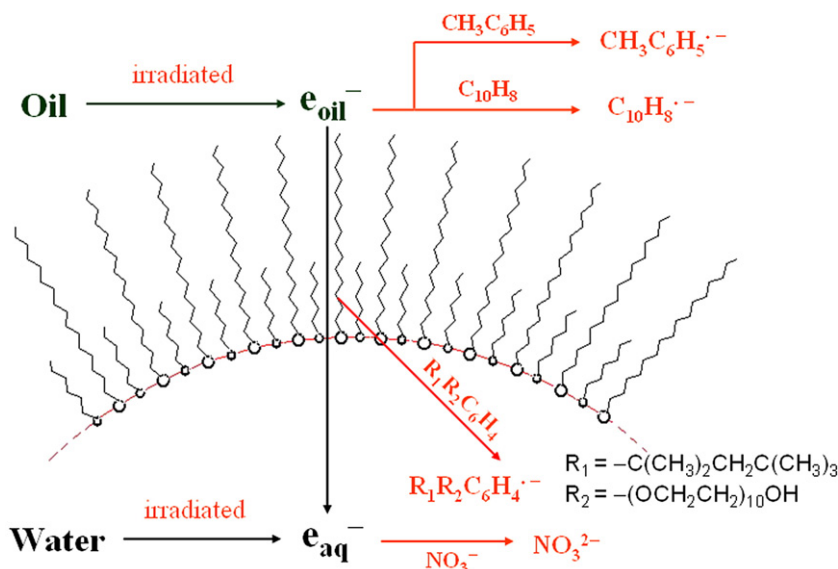


Fig. 4. Schematic illustration of the generation, migration and quenching of electrons in W/O microemulsions.

$e_{aq}^-$  play a key role. The idea for controlling the radiolytic syntheses of NPs was realized.

With the increase of the  $\omega$  value from 4.5 to 7.0, the yield of  $e_{aq}^-$  is increased, leading to the transformation of the reduction product of  $\text{Cu}(\text{NO}_3)_2$  from  $\text{Cu}_2\text{O}$  to Cu in Brij 30-based microemulsions (Table 3) [74].

Because  $e_{aq}^-$  is mainly generated from the scavenging of solvated electron in oil phase ( $e_{oil}^-$ ) by water pool, the concentration of  $e_{aq}^-$  in water pool will decrease if  $e_{oil}^-$  is scavenged by some groups during its migration into water pool, i.e., the aromatic ring in toluene, naphthalene or Triton X-100 (Fig. 4). This does not favor the further reduction of  $\text{Cu}^+$  by  $e_{aq}^-$  and is therefore propitious to the formation of  $\text{Cu}_2\text{O}$ . Because there is no aromatic ring in the molecular structure of Brij 56, under the identical  $\omega$  value, the concentration of  $e_{aq}^-$  in the water pool of the Brij 56-based microemulsion is higher than that in the Triton X-100-based microemulsion. So the reduction product of  $\text{CuSO}_4$  in Brij 56 system is Cu, while it is  $\text{Cu}_2\text{O}$  in Triton X-100 system (Table 3) [74]. When toluene or naphthalene is added to Brij 56 system, the reduction product of  $\text{CuSO}_4$  can be transformed from Cu to  $\text{Cu}_2\text{O}$  [74].

As the rate constant of the reaction between  $e_{aq}^-$  and  $\text{NO}_3^-$  ( $9.7 \times 10^9 \text{ Lmol}^{-1} \text{ s}^{-1}$ ) is much higher than those of other reactions between  $e_{aq}^-$  and  $\text{Cl}^-$  (or  $\text{SO}_4^{2-}$ ) ( $< 1.0 \times 10^6 \text{ Lmol}^{-1} \text{ s}^{-1}$ ) [32],  $\text{NO}_3^-$  can scavenge  $e_{aq}^-$  and decrease its yield effectively, while the abilities of  $\text{SO}_4^{2-}$  and  $\text{Cl}^-$  are much weaker. Although the rate constant of the reaction between  $e_{aq}^-$  and  $\text{Br}^-$  is short, it is logical to extrapolate that the ability of  $\text{Br}^-$  and  $\text{Cl}^-$  to scavenge  $e_{aq}^-$  is similar because of their similar nature. Thus, in Brij 56 system, the reduction product of Cu

( $\text{NO}_3$ )<sub>2</sub> is  $\text{Cu}_2\text{O}$ , while those of  $\text{CuSO}_4$ ,  $\text{CuCl}_2$  and  $\text{CuBr}_2$  are Cu (Table 3) [74].

Besides the effect on the chemical composition, anions can also affect the morphology of the reduction product of  $\text{Cu}^{2+}$ . In Brij 30 system, the morphologies of the reduction products of  $\text{Cu}^{2+}$  are much different (Fig. 5) [74]. The aspect ratio of rod-like Cu NPs obtained from  $\text{Cu}(\text{NO}_3)_2$  is obviously larger than those obtained from  $\text{CuSO}_4$  and  $\text{CuCl}_2$ , and there seldom appear rod-like Cu NPs when  $\text{CuBr}_2$  is used as precursor [74]. This phenomenon could not be explained by the preferential adsorption of anion on some crystal faces of NPs [51,75], and may be ascribed to the strongest effect of  $\text{NO}_3^-$  on the yield of  $e_{aq}^-$  [74]. It is known that different crystal faces of NCs have different growing rates. This difference is obvious when the generation rate of NCs is slow enough. In this system,  $\text{NO}_3^-$  may reduce the yield of  $e_{aq}^-$  and thus the rate of reduction to such an extent that the difference of the growing rates between different crystal faces is large enough to form Cu nanorod in Brij 30 system [74]. It is suggested that the morphology of reduction product may be controlled by the yield of  $e_{aq}^-$  [74].

#### 2.4.2. Radiolytic syntheses of octahedral $\text{Cu}_2\text{O}$ nanocrystals

In Triton X-100-based microemulsion, with  $\text{Cu}(\text{NO}_3)_2$  as precursor, octahedral  $\text{Cu}_2\text{O}$  NCs smaller than 100 nm were successfully obtained by  $\gamma$ -irradiation (Fig. 6A and Table 4) [76]. Meanwhile, there was no Cu generated in the course of irradiation [76]. When the dose rate increased from 22.7 to 92.2 Gy/min, the average edge length of the octahedral  $\text{Cu}_2\text{O}$  NCs varied from 95 to 45 nm [76]. In the absorption spectra, the characteristic absorption peaks of  $\text{Cu}_2\text{O}$  were blue-shifted. As the dose rate increased to 132.0 Gy/min, only quasi-spherical NPs with diameter of ca. 3 nm but no other shaped NPs could be found [76]. This is believed to be the results of the competition between the aggregation mechanism and the diffusion mechanism [76]. Because the  $\text{Cu}_2\text{O}$  is derived from the hydrolysis of  $\text{Cu}^+$ , which is generated via the reduction of  $\text{Cu}^{2+}$  by  $e_{aq}^-$ , the generation rate of  $\text{Cu}_2\text{O}$  increases with the increase of the concentration of  $e_{aq}^-$ . When the dose rate is higher, the concentration of  $e_{aq}^-$  is higher, the degree of supersaturation of  $\text{Cu}_2\text{O}$  is higher, there are more crystal nuclei generated, and the aggregation mechanism overwhelms the diffusion mechanism, so  $\text{Cu}_2\text{O}$  forms mainly polycrystals; in contrast, when the dose rate becomes lower, the  $\text{Cu}_2\text{O}$  single crystals are formed [76].

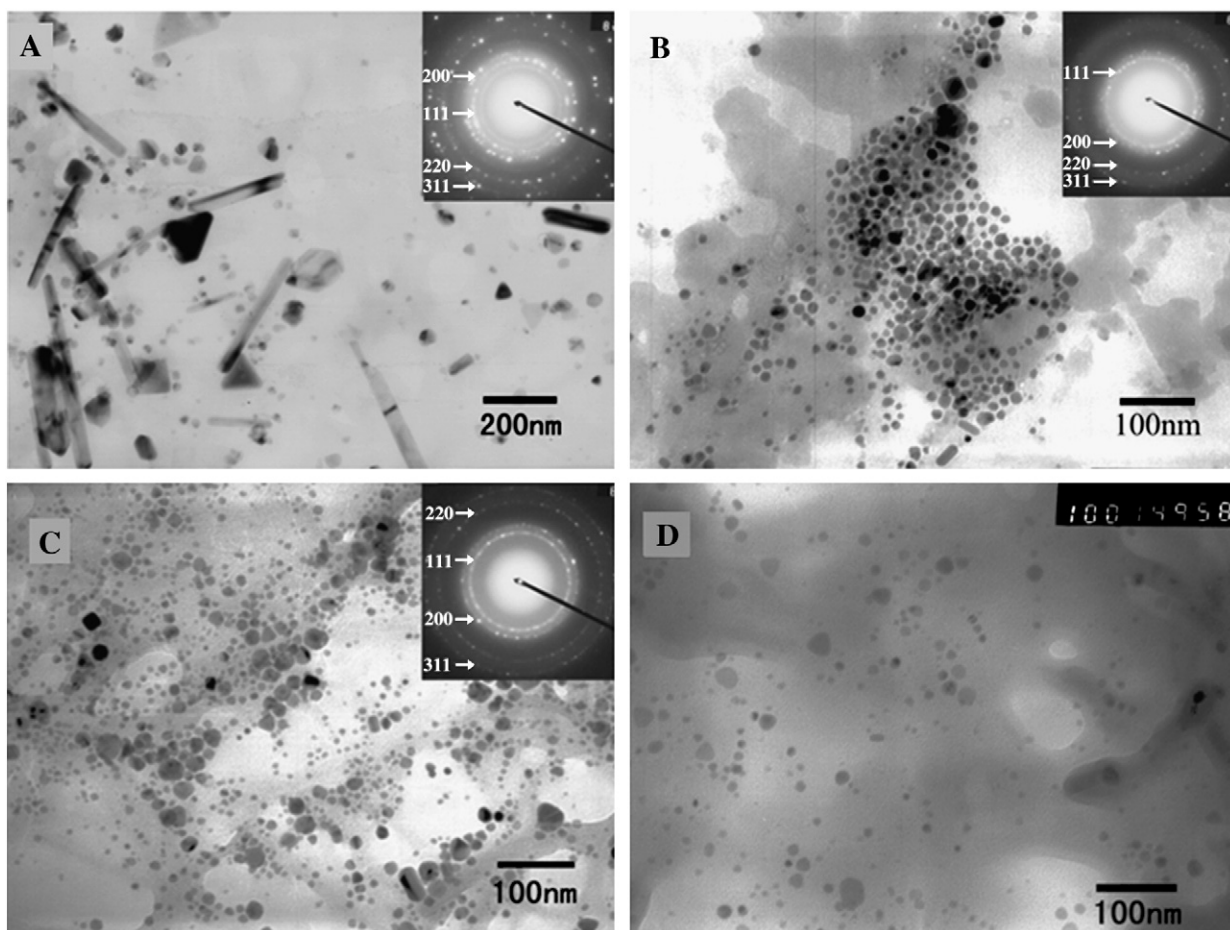
It may be the combined action of  $\text{NO}_3^-$  and the phenyl ring in Triton X-100 that reduce the yield of  $e_{aq}^-$  and thus the rate of reduction to such an extent. This favors the preferential crystal growth along the

Table 3  
Summary of the reduction products of  $\text{Cu}^{2+}$  under different conditions.<sup>a</sup>

Surfactant	$\omega$	$\text{Cu}(\text{NO}_3)_2$	$\text{CuSO}_4$	$\text{CuCl}_2$	$\text{CuBr}_2$
Triton X-100	9.0	$\text{Cu}_2\text{O}$	$\text{Cu}_2\text{O}$	Cu	Cu
	12.0	$\text{Cu}_2\text{O}$	–	–	–
Brij 56	9.0	$\text{Cu}_2\text{O}$	Cu	Cu	Cu
Brij 30	4.5	$\text{Cu}_2\text{O}$	–	–	–
	5.4	$\text{Cu}_2\text{O}$ and Cu	–	–	–
	6.0	Cu	–	–	–
	7.0	Cu	Cu	Cu	Cu

Triton X-100,  $(\text{CH}_3)_3\text{CCH}_2\text{C}(\text{CH}_3)_2\text{C}_6\text{H}_4(\text{OCH}_2\text{CH}_2)_n\text{OH}$  ( $n=9-10$ ); Brij 56,  $\text{CH}_3-(\text{CH}_2)_{14}\text{CH}_2(\text{OCH}_2\text{CH}_2)_{10}\text{OH}$ ; Brij 30,  $\text{CH}_3(\text{CH}_2)_{10}\text{CH}_2(\text{OCH}_2\text{CH}_2)_4\text{OH}$ .

<sup>a</sup> Taken from Ref. [74].



**Fig. 5.** TEM images of the reduction products of  $\text{Cu}^{2+}$  in Brij 30-based microemulsions ( $\omega = 7.0$ ) by  $\gamma$ -irradiation in the presence of different precursors: (A)  $\text{Cu}(\text{NO}_3)_2$ , (B)  $\text{CuSO}_4$ , (C)  $\text{CuCl}_2$ , (D)  $\text{CuBr}_2$ . The insets show the SAED patterns of the corresponding products. Taken from Ref. [74].

$\langle 100 \rangle$  direction and makes the rate far exceed that along  $\langle 111 \rangle$ , thus  $\{100\}$  faces shrink and  $\{111\}$  face is formed. Then, octahedral  $\text{Cu}_2\text{O}$  NCs were obtained in Triton X-100-based microemulsion when  $\text{Cu}(\text{NO}_3)_2$  was used as precursor (Fig. 6A and Table 4) [76]. While in Brij 56-based microemulsion, only the  $\text{NO}_3^-$  can scavenge  $e_{\text{aq}}^-$ . Thus, the yield of  $e_{\text{aq}}^-$  and the generation rate of  $\text{Cu}_2\text{O}$  are higher than those in Triton X-100 system, respectively, which favor the preferential crystal growth along the  $\langle 111 \rangle$  direction and make the rate far exceed that along  $\langle 100 \rangle$ . Thus,  $\{111\}$  faces shrink and  $\{100\}$  face is formed. Then, the  $\text{Cu}_2\text{O}$  nanocubes were obtained (Fig. 6B and Table 4) [74].

Before our work, although octahedral  $\text{Cu}_2\text{O}$  crystals have been reported in the literature, their edge length was larger than 350 nm [77,78]. Thus, to the best of our knowledge, this is the first report about the syntheses of octahedral  $\text{Cu}_2\text{O}$  NCs. Later, considerable efforts were continuously paid to the formation, shape evolution and properties of octahedral  $\text{Cu}_2\text{O}$  NCs with different sizes [79–85]. Especially, Xu et al. [81] found that the octahedral  $\text{Cu}_2\text{O}$  NCs with exposed  $\{111\}$  crystal surfaces possess much higher activity on adsorption and photodegradation of methyl orange than cubic  $\text{Cu}_2\text{O}$  particles. Moreover, with the decrease of the edge length, the octahedral  $\text{Cu}_2\text{O}$  particles exhibited much higher activities [81]. Therefore, octahedral  $\text{Cu}_2\text{O}$  NCs are promising candidates for the treatment of organic pollutions.

Among the approaches, routine chemical methods, such as adjusting pH, temperature, molar ratio of reactants and selecting different additives and reductants, were often used in solutions to affect the growth of different crystal faces. However, the size of the octahedral  $\text{Cu}_2\text{O}$  NCs was always larger than 100 nm. Cu NPs were obtained via routine chemical reduction in the Triton X-100-based microemulsion [86]. This indicates that the mechanism of radiolytic reduction is

obviously different from that of the routine chemical reduction, and the combination of ionizing radiation and microemulsion can afford us more unique conditions to control the morphology and size of NPs.

#### 2.4.3. Radiolytic syntheses of solid and hollow $\text{Cu}_2\text{O}$ nanocubes

In the further work conducted to confirm the morphology control of the reduction products by the yield of  $e_{\text{aq}}^-$ , Triton X-100 and Brij 56 were selected to construct W/O microemulsions with *n*-hexanol, cyclohexane and aqueous solution of  $\text{Cu}(\text{NO}_3)_2$  in the presence of ethylene glycol (EG) [87]. In the two systems, the effects of the  $\omega$  value and  $\text{NO}_3^-$  on the yield of  $e_{\text{aq}}^-$ , and the effect of EG on the viscosity of the water pool should be similar to a great extent because the components, except the surfactant, and their contents of the two microemulsions were the same. The obvious difference was the phenyl ring in Triton X-100. In the Triton X-100-based microemulsion, local ordered structure constructed by solid  $\text{Cu}_2\text{O}$  nanocubes was obtained by the radiolytic reduction of  $\text{Cu}(\text{NO}_3)_2$  (Fig. 6C and Table 4) [87]. However, when Triton X-100 was replaced by Brij 56 in the microemulsion, hollow  $\text{Cu}_2\text{O}$  nanocubes were synthesized (Fig. 6D and Table 4) [87]. The addition of toluene into the Brij 56 system could decrease the ratio of hollow nanocubes [87]. It was suggested that the balance between the reduction rate of  $\text{Cu}^{2+}$  depending on the yield of  $e_{\text{aq}}^-$  and the escape rate of the mixed solvent determined their final morphologies. In the Brij 56-based microemulsion, due to the absence of phenyl ring, the yield of  $e_{\text{aq}}^-$  and its generation rate are higher than those in the Triton X-100-based microemulsion. Thus, the mixed solvent could not escape as soon as possible and may be encapsulated in the interior of the generated  $\text{Cu}_2\text{O}$  NPs. During the process of ripening or post treatments, the encapsulated solvent would gradually escape, leading to the formation of hollow structure [87].



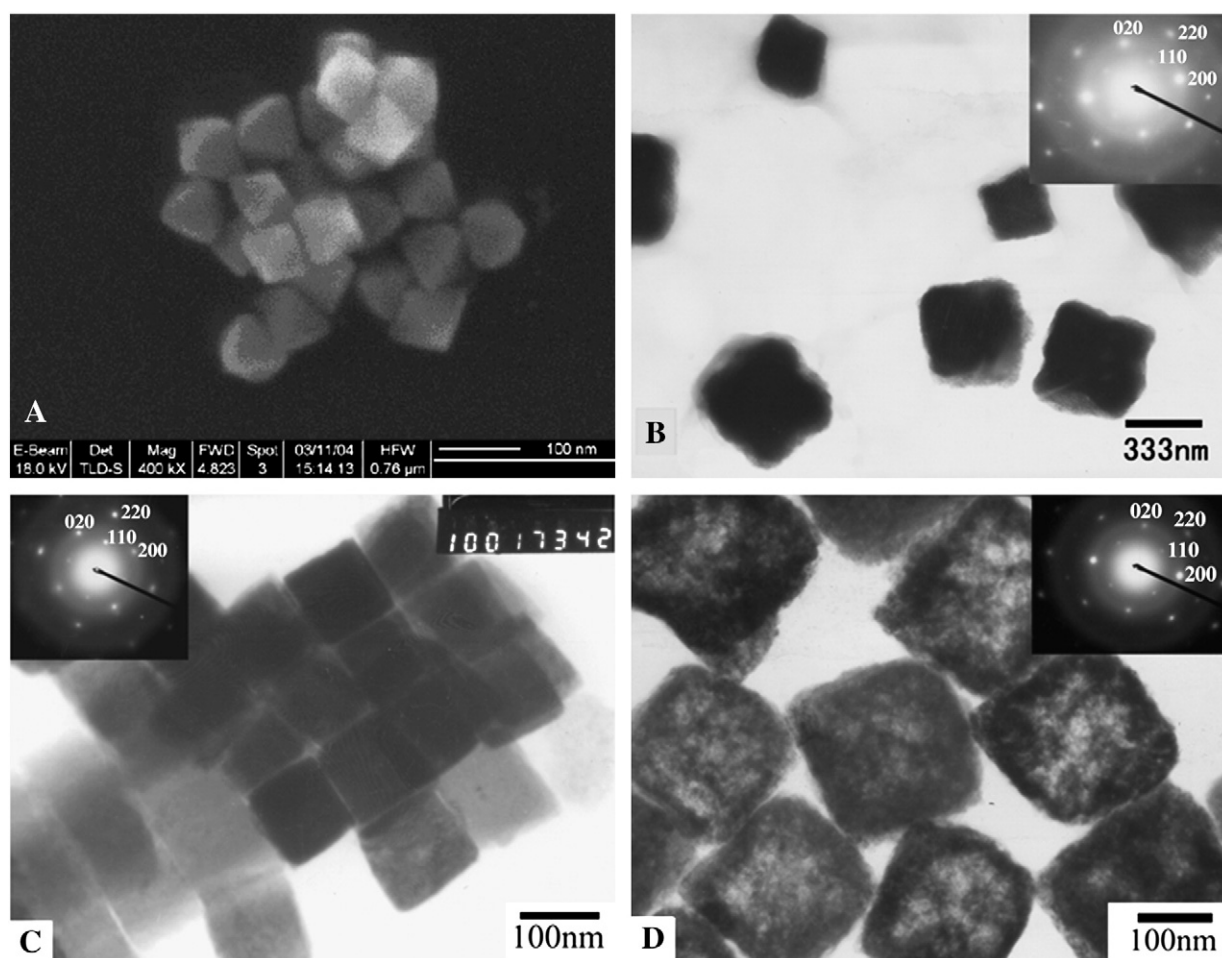


**Fig. 6.** SEM (A) and TEM (B–D) images of the reduction products of  $\text{Cu}(\text{NO}_3)_2$  in Triton X-100 (A and C) and Brij 56 (B and D) based microemulsions ( $\omega = 9.0$ ) by  $\gamma$ -irradiation in the absence (A and B) and presence (C and D) of ethylene glycol. Taken from Refs. [76], [87] and [74].

In the growth process of  $\text{Cu}_2\text{O}$  NPs, there is a mass exchange course between water pools. The presence of EG can reduce the rigidity of the interface of a W/O microemulsion, which favors the mass exchange. Besides, the presence of EG can also increase the viscosity of the water pool obviously, which reduces the reactivity of  $e_{\text{aq}}^-$  similar to the situation in AOT-based microemulsion. In the Brij 56-based microemulsion with EG, although the reactivity of  $e_{\text{aq}}^-$  is reduced to a certain extent, the rate of mass exchange between water pools is increased. It might be the latter effect that plays an important role, enhancing the growth rate of  $\text{Cu}_2\text{O}$  NPs and leading to the formation of hollow nanocubes [87]. In contrast, solid nanocubes are finally formed in the Brij 56-based microemulsion without EG (Fig. 6B and Table 4) [74]. However, in the Triton X-100-based microemulsions, the addition of EG only makes the morphology of  $\text{Cu}_2\text{O}$  change from octahedral NCs to nanocubes. Although the rigidity of the interface is reduced in the presence of EG, the yield of  $e_{\text{aq}}^-$  and its generation rate in this system are so low that the polar solvent can escape in time. This may be the reason that the nanocubes are solid despite of the existence of EG [87].

**Table 4**  
Comparison of the morphologies of  $\text{Cu}_2\text{O}$  NCs synthesized in the Triton X-100 and Brij 56 based microemulsions both with and without ethylene glycol (EG).<sup>a</sup>

Surfactant	Without EG	With EG
Triton X-100	Octahedral NCs, solid [76]	Nanocubes, solid [87]
Brij 56	Nanocubes, solid [74]	Nanocubes, hollow [87]

<sup>a</sup> Taken from Ref. [87].

As to the shape transformation, it may be related to the adsorption of EG on the special surfaces of  $\text{Cu}_2\text{O}$  NPs [87].

According to the work of Yang et al. [88],  $\text{Cu}_2\text{O}$  nanocubes possess photovoltaic characteristics, which may be useful for the fabrication of photoelectronic devices. In addition, Tang et al. [89] found that  $\text{Cu}_2\text{O}$  nanocubes could catalyze the N-arylations reaction of nitrogen-containing heterocycles with aryl and heteroaryl halide in high efficiency.

#### 2.5. Research on the growth kinetics of nanoparticles in microemulsion by ionizing radiation

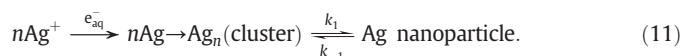
The study of growth kinetics is always active because a better understanding on the growth of NPs will favor the rational synthesis manipulation [90–92]. In the literature, pulse radiolysis has been applied to investigate the reduction of  $\text{Au}^+$  [93],  $\text{Ag}^+$  [28,30],  $\text{Cu}^{2+}$  [94],  $\text{Ti}^+$  [95],  $\text{Cd}^{2+}$  [96],  $\text{Ni}^{2+}$  [97],  $\text{Pb}^{2+}$  [98] and  $\text{Pd}^{2+}$  [99] in aqueous solution, and the formation of colloid metal, which play an important role in the development of nanoscience and nanotechnology. In microemulsions, pulse radiolysis is also important in this field. In a PEGDE-based microemulsion, Fendler et al. [52] investigated the reduction of  $\text{Au}^{3+}$  and the formation of Au NPs. In a SDS-based microemulsion, Kapoor et al. [56] found the formation of  $\text{Ag}_3^{2+}$  in the growth process of Ag NPs. This is the first report about this kind of Ag cluster. In the experiment of pulse radiolysis, electron beam is used and the dose rate is very high, and ultrafast detection is required.

In the radiolytic syntheses of NPs with low dose rate, the generation rate of the reducing species is so slow that the duration of the growth course is longer, and normal detection methods can be applied. In



addition, the reducing species are generated with uniform speed and their concentration is almost constant in the course of irradiation. Thus, the ionizing radiation with low dose rate should also be suitably used to investigate the growth kinetics of NPs, which was not noticed before. As well known, noble metal (such as Ag and Au) clusters and small NPs exhibit fascinating fluorescence or photoluminescence characteristics, while the bigger ones do not [1,100,101]. Moreover, Ag clusters and NPs have corresponding absorption peaks, respectively [28,30]. Therefore, we took full advantage of the spectra characteristics and irradiation technique to explore the growth kinetics of Ag NPs [102].

In the W/O microemulsion composed of SDS, *n*-hexanol, cyclohexane and aqueous solution of AgNO<sub>3</sub>, Ag NPs were synthesized by  $\gamma$ -irradiation [102]. The absorption spectra in different formation stages indicated the coexistence of Ag cluster and NPs. At the same dose rate, with the increase of irradiation time, the absorption peak corresponding to Ag cluster became weaker gradually, while the peak related to Ag NPs became stronger. Furthermore, the photoluminescence spectra in different formation stages also exhibited that the intensity of the emission peak became weaker with the increase of irradiation time. Then, a possible mechanism (Eq. (11)) was proposed: at first, only nonmetallic clusters with less number of Ag atoms are formed; then, these clusters become larger clusters or NPs by aggregation and/or further reduction of Ag<sup>+</sup> on their surface [102]. Meanwhile, a reversible equilibrium exists between clusters and NPs (Eq. (11)).



The values of  $k_1 + k_{-1}$  were determined to be  $(1.60 \pm 0.16) \times 10^{-2} \text{ s}^{-1}$  and  $(1.54 \pm 0.42) \times 10^{-2} \text{ s}^{-1}$  by the nonlinear regression analyses for

the data from the absorption and photoluminescence spectra vs. time, respectively [102].

### 3. Radiolytic syntheses of nanoparticles in other supramolecular assemblies

#### 3.1. Radiolytic syntheses of nanoparticles controlled by cyclodextrins

In the realm of nanoscience and nanotechnology, it is known that thiolated CDs and the inclusion complexes of CDs and thiol compounds can be used to stabilize NPs and further construct supramolecular nanostructures [103–106]. More interestingly, non-thiolated CDs can also be used to protect NPs independently, which are regarded as a sort of characteristic protective agents for the preparation of water-soluble NPs [107]. So far, besides CdS [108], CuS [109], TiO<sub>2</sub> [110] and Fe<sub>3</sub>O<sub>4</sub> [111–113] NPs, water-soluble Au [114–121], Ag [122], Au–Ag [123], Ru [107,124], Rh [125] and Pd [126] metal NPs have been synthesized with the assistance of non-thiolated CDs. Meanwhile, there appear some novel supramolecular phenomena. For instance, in a biphasic liquid–liquid system, because of the formation of inclusion complexes of aromatic compounds and methylated CDs (Me-CDs), aromatic compounds could be transported from oil phase to aqueous solution, and be hydrogenated on the surfaces of water-soluble Ru NPs protected by Me-CDs [107,124]. As the interaction between aromatic compounds and Me-CDs was stronger than that between the corresponding reduction products and Me-CDs, the reduction products were released to oil phase in time [107,124]. Thus, the efficiently catalytic hydrogenation of aromatic compounds was realized conveniently [107,124]. Ng et al. [122] found that the  $\alpha$ -CDs aligned on the surface of Ag NPs could lead to

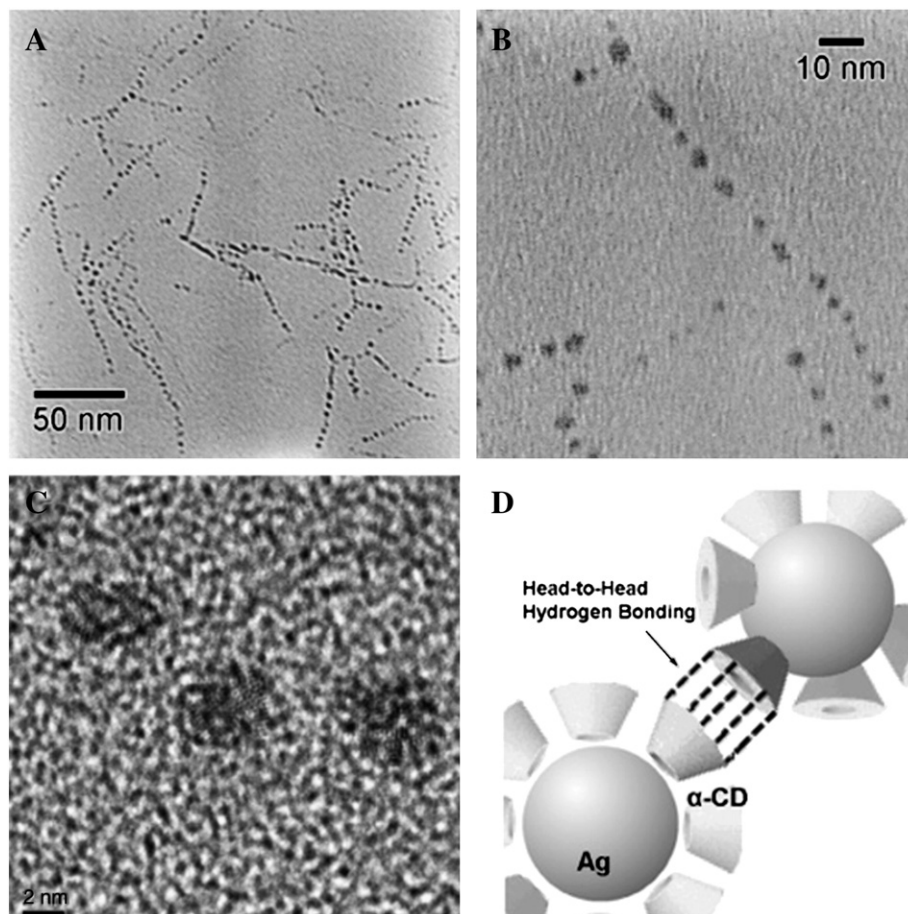


**Fig. 7.** (A and B) TEM images illustrating the self-assembly of Ag NPs into 1-D pearl necklace arrays. (C) HRTEM image of the Ag NPs revealing their crystallinity. (D) Schematic of the hydrogen-bonding interactions between the secondary-OH groups on the surface-attached CD (not drawn to scale). Taken from Ref. [122].

the formation of one-dimensional pearl necklace arrays of Ag NPs through the hydrogen-bonding interactions between the exposed secondary hydroxyl groups (Fig. 7).

With respect to the interaction between CDs and NPs, there are two opinions. One opinion is that the stabilization of the NPs was achieved by hydrophobic interactions (or inclusion-complexation interaction) between CDs and NPs [108,114,122,124,125], the other opinion considers that CDs adsorb on the surface of NPs through their hydroxyl groups and protect NPs [109,111,116]. The divergence between them is focused on whether the hydroxyl groups interact with NPs or not. As to the former, because the size of NPs is much larger than the diameter of the cavity, it is difficult to image the formation of inclusion complexes. Recently, it has been observed that non-inclusion complexes can also participate in the CD solubilization of poorly soluble drugs [127]. At low CD concentrations (at about 1%, w/v) the fraction of CD molecules forming aggregates is insignificant but the aggregation increases rapidly with increasing CD concentration [127]. Also, formation of CD complexes can increase the tendency of CDs to form aggregates and can lead to formation of micellar-type CD aggregates capable to solubilize poorly soluble drugs that do not readily form inclusion complexes [127]. In the former opinion, the NPs should be similar to the poorly soluble drugs. Up to now, two opinions are still waiting the strong evidence from experiments.

When the aqueous solutions containing CDs is irradiated by ionizing radiation, it is the  $\cdot\text{OH}$  that extract the H atoms of the hydroxyl group on C1 and C5 positions, while the reaction between  $e_{aq}^-$  and CDs is relatively weak. As the absorbed dose goes beyond some extent, CDs will be decomposed [128–130]. Therefore, the controlled reduction of  $\text{Cu}^{2+}$  took place within the safe absorbed dose. With the increase in the concentration of  $\beta$ -CD, the reduction product of  $\text{Cu}(\text{NO}_3)_2$  could be gradually transformed from  $\text{Cu}_2\text{O}$  to Cu [131]. When the concentration of  $\beta$ -CD increased to  $8.0 \times 10^{-3} \text{ mol L}^{-1}$ , the reduction product was composed of pure Cu NPs [131]. This was the first report on the preparation of light transition metal NPs with the assistance of non-thiolated CDs. In the course of irradiation, there was no  $\text{Cu}_2\text{O}$  generated [131]. It was attributed to the regularity that  $\beta$ -CD is able to scavenge  $\cdot\text{OH}$ , which suppresses the reaction between  $e_{aq}^-$  and  $\cdot\text{OH}$ , and increases the yield of  $e_{aq}^-$ . This favors the generation of Cu [131].

As a typical light transition metal, Cu NPs were easy to be oxidated by water in the absence of protective agents and  $\text{Cu}_2\text{O}$  NPs were always obtained [86]. In our research, this radiolytically synthesized Cu NPs were stable under  $\text{N}_2$  atmosphere, while they were gradually oxidated to CuO NPs in the air [131]. Thus, the Cu NPs should be stabilized in a hydrophobic circumstance, such as the core of the micellar-type CD aggregates. However, this circumstance could not prevent the oxidation of Cu NPs by  $\text{O}_2$ .

It is known that the formation of NPs and the sterilization can take place simultaneously [132], and CDs have been widely used in the field of biomedicine. Therefore, it is reasonable to believe that the radiolytic syntheses of NPs in the presence of CDs will be an efficient and facile way in the preparation of NPs for biomedical application in the future.

### 3.2. Radiolytic syntheses of nanoparticles in ionic liquids

Because the obtained inorganic NPs are stable in ILs without the assistance of stabilizers and bare NPs show high catalytic activities, ILs have been attracted much attention in the realm of nanoscience and nanotechnology [22–24]. It is always considered that ILs themselves act as stabilizers [24]. Indeed, they are able to isolate NPs and prevent aggregation, due to their characteristics of supramolecular structure in microdomains [26].

Similar to the normal molecular solvents, macroscopically, ILs are homogeneous except some improved properties. In fact, with respect to imidazolium ILs, the typical and most popular ILs, there exists a supramolecular network of cations and anions connected together by hydrogen bonding (Fig. 8A) in solid state [25,26]. Besides, other

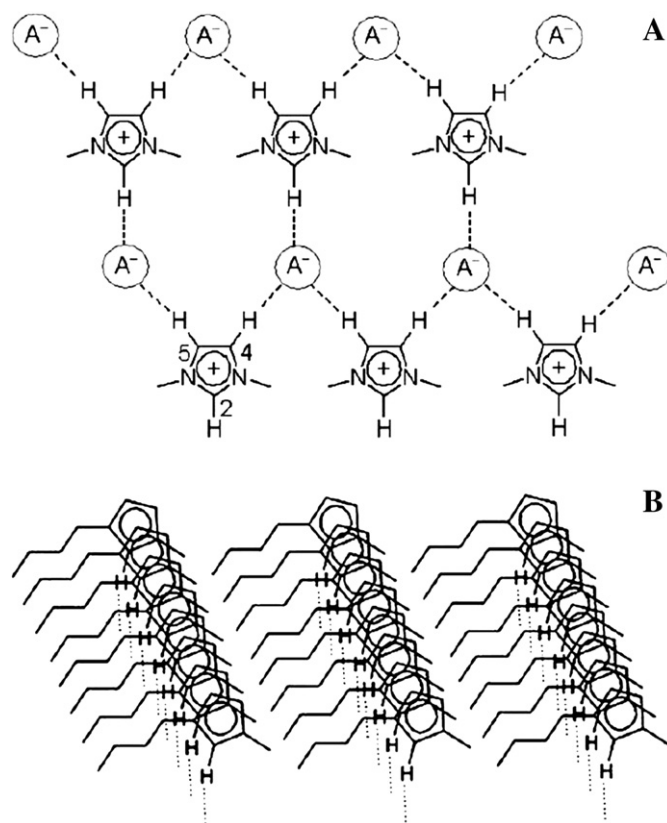


Fig. 8. Simplified two- (A) and three-dimensional (B) supramolecular structures of imidazolium ILs. Taken from Ref. [26].

interactions (such as electrostatic interactions,  $\pi$ - $\pi$  stacking, C-H- $\pi$  interactions and combination of these interactions) between the cations and the anions can also lead to the formation of the supramolecular network [25,26]. Furthermore, the above two-dimensional organization may evolve to three-dimensional structures through the chains of imidazolium rings (Fig. 8B) [25,26]. In some cases, there are  $\pi$ - $\pi$  stacking interactions among imidazolium rings, and a relatively weak C-H- $\pi$  interactions via the methyl group and the  $\pi$  system of the imidazolium ring in 1-alkyl-3-methylimidazolium salts can also be found [25,26].

When ILs are transformed from crystal to liquid state, the long-range order is lost, but long-range Coulomb interactions between cations and anions of the ILs are maintained. It is the long-range Coulomb interactions in ILs that can lead to longer spatial correlations than those in classic van der Waals organic liquids. In other words, the supramolecular structures observed in crystal are reserved in liquid state [25,26]. Furthermore, in 1-alkyl-3-methylimidazolium ILs ( $n \geq 4$  in  $\text{C}_n$ ), there also exist polar domains, formed by the head groups of the cations and anions, and non-polar domains, formed by the alkyl groups [133–135]. It is considered that the synthesized NPs are included in the supramolecular network with polar and non-polar regions without aggregation [26].

Pulse radiolysis work has demonstrated the formation of solvated electrons and radicals in some ILs in the course of irradiation [136–141]. It is believed that this type of solvated electrons and radicals, acting like  $e_{aq}^-$  and those radicals in water, can reduce precursors to low valence and lead to the formation of NPs. Recently, Imanishi et al. [142] obtained Au NPs in 1-butyl-3-methylimidazolium bis(trifluoromethanesulfonyl)imide ( $[\text{C}_4\text{mim}][\text{Tf}_2\text{N}]$ ) IL by low-energy electron beam irradiation. Furthermore, for the first time, Tsuda et al. [143] successfully established a large-scale production method for stable NPs without any stabilizing agents (Fig. 9). In this method, they synthesized Au NPs at an absorbed

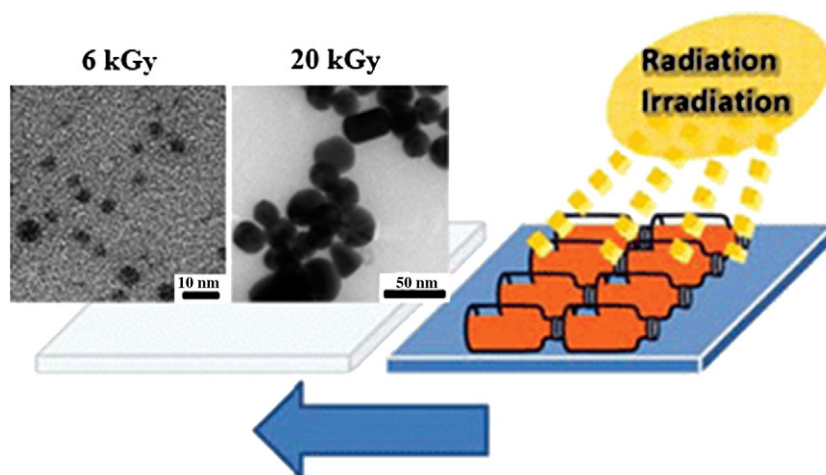
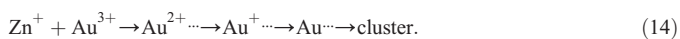


Fig. 9. Scheme of the large-scale preparation of Au NPs in ILs by ionizing radiation, and the TEM images of the Au NPs synthesized at the absorbed doses of 6 and 20 kGy. Taken from Ref. [143].

dose of 6 kGy in  $[C_4mim][Tf_2N]$  IL by  $\gamma$ -ray and accelerated electron beam irradiations. As the absorbed dose increased to 20 kGy, the size of the obtained Au NPs became larger (Fig. 9). Therein, the obtained Au NPs were stable without the assistance of additional stabilizers for more than three months. However, in tributylmethylammonium bis-(trifluoromethanesulfonyl)imide ( $[Bu_3MeN][Tf_2N]$ ) IL, no Au NPs generated at an absorbed dose of 20 kGy. This phenomenon may be ascribed to the regularity that imidazolium-based ILs release reactive species much more easily than non-heterocyclic ammonium-based ILs [139–141,143,144].

In a special quaternary ammonium-based IL (QAIL),  $[Me_3NC_2H_4OH][Zn_2Cl_5]$ , Wu et al. [145] realized the radiolytic reduction of Au (III) and the formation of Au NPs. They suggested that  $Zn^{2+}$  play an important role in the reduction of Au (III) (Eqs. (12)–(14)). They also found that the size of the Au NPs can be varied between 10 and 50 nm by changing the medium composition, i.e., the volume ratios of QAIL to 2-propanol (or water) [145]. Therefore, the medium composition can be used to control the synthesis and the size of NPs. Without doubt, the application of ILs will make the radiolytic synthesis of NPs more abundant because the physical–chemical properties of ILs can be conveniently adjusted through altering the kinds of cations and anions.



#### 4. Conclusions and prospects

Ionizing radiation is a powerful method in the synthesis of NPs and nanostructures. The application of ionizing radiation on supramolecular assemblies can afford us unique conditions to control the composition and morphology of NPs.

In microemulsion, it has been proved that the effects of many conditions on the yield of  $e_{\text{aq}}^-$  play a key role, remarkably different from the mechanism in routine chemical method. For example, the compounds with aromatic ring could be used to control the syntheses of NPs, which is difficult to be realized in routine chemical method. Moreover, anions, especially  $NO_3^-$ , can affect the composition and morphology of NPs *via* its effect on the yield of  $e_{\text{aq}}^-$ , obviously different from the mechanism in routine chemical method. Simultaneously, *via* the controlled syntheses of NPs, the mechanism concerning the

producing of  $e_{\text{aq}}^-$  in microemulsion was well exhibited. However, the application and validation of this regularity are confined in the reduction of  $Cu^{2+}$ . It is necessary to extend its application fields and make the controlled synthesis of NPs more free. Moreover, in other supramolecular assemblies consist of surfactants (e.g., liquid crystals and vesicles), there also exist many regularities of radiation chemistry, such as dual solvation sites of the radiolytically generated electrons in liquid crystals [146]. The application of these regularities will contribute in a novel and rational way to understand the formation of NPs and to prepare NPs with special morphology and function in these systems. In addition, ionizing radiation with low dose rate is suitable to investigate the growth kinetics of NPs. How to extend its research object? This is also a subject with challenge.

$\beta$ -CD has been proved to be useful in the radiolytic syntheses of water-soluble Cu NPs. This is only the beginning in the field, more CDs and CD-based assemblies will be used to prepare novel water-soluble NPs by ionizing radiation, which contribute in a new way to the preparation of NPs for biomedical application in the future. Luong et al. [114] have ever speculated that single gold atoms or clusters may be enclosed in the CD cavity to form an inclusion complex, which has not been proved by experiment. Because pulse radiolysis is powerful in the study of reduction kinetics of metal ions, especially in the investigation of the formation of nanoclusters, it can be used to confirm or negate the speculation, and afford us useful information about the interaction between CDs and NPs.

With respect to the radiolytic preparation of NPs in ILs, although some progress has been made, it is still in its early stage. Up to now, only Au NPs were obtained. There is still challenge in this field. Besides, the application of ionizing radiation in ILs should play an important role in controlling the morphology of NPs and nanostructures because many ILs can form thermotropic liquid crystals [27] or take part in the formation of supramolecular assemblies [26,147–149], e.g., microemulsions, lyotropic liquid crystals and liquid clathrates.

Considering the advantages of the radiation technique and the unique natures of supramolecular assemblies, there is promise for a convenient strategy for the controlled preparation of NPs using this combinatorial approach.

#### Abbreviations

AOT	sodium bis-(2-ethylhexyl)sulfosuccinate
Brij 30	tetraethylene glycol dodecyl ether [CH <sub>3</sub> (CH <sub>2</sub> ) <sub>10</sub> CH <sub>2</sub> (OCH <sub>2</sub> CH <sub>2</sub> ) <sub>4</sub> OH]
Brij 56	decaethylene glycol hexadecyl ether [CH <sub>3</sub> (CH <sub>2</sub> ) <sub>14</sub> CH <sub>2</sub> (OCH <sub>2</sub> CH <sub>2</sub> ) <sub>10</sub> OH]
$[Bu_3MeN]^+$	methyl tributylammonium



CD(s)	cyclodextrin(s)
[C <sub>4</sub> mim] <sup>+</sup>	1-butyl-3-methylimidazolium
EB	electron beam
HEC	hydroxyethyl cellulose
IL(s)	ionic liquid(s)
Me-CDs	methylated cyclodextrins
[Me <sub>3</sub> NC <sub>2</sub> H <sub>4</sub> OH] <sup>+</sup>	hydroxyethyl trimethylammonium
NCS	nanocrystals
NPs	nanoparticles
OP-10	octylphenyl poly(ethylene glycol) ether ( <i>n</i> = 10)
OP-4	octylphenyl poly(ethylene glycol) ether ( <i>n</i> = 4)
PEGDE	pentaethylene glycol dodecyl ether
QAIL	quaternary ammonium-based IL
SDBS	sodium dodecyl benzene sulfonate
SDS	sodium dodecyl sulfate
[Tf <sub>2</sub> N] <sup>-</sup>	bis(trifluoromethanesulfonyl)imide
Triton X-100	4-(1,1,3,3-tetramethylbutyl)phenyl poly(ethylene glycol) ether ( <i>n</i> = 9–10) [(CH <sub>3</sub> ) <sub>3</sub> CCH <sub>2</sub> C(CH <sub>3</sub> ) <sub>2</sub> C <sub>6</sub> H <sub>4</sub> (OCH <sub>2</sub> CH <sub>2</sub> ) <sub><i>n</i></sub> OH]

## Acknowledgments

This work was supported by the National Natural Science Foundation of China (Grants 29901001 and 20871009) and the Coordinated Research Projects of International Atomic Energy Agency (Research Contract No: 15107).

## References

- Burda C, Chen XB, Narayanan R, El-Sayed MA. *Chem Rev* 2005;105:1025.
- Roucoux A, Schulz J, Patin H. *Chem Rev* 2002;102:3757.
- Alivisatos AP. *Science* 1996;271:933.
- Sun YG, Xia YN. *Science* 2002;298:2176.
- Tian N, Zhou ZY, Sun SG, Ding Y, Wang ZL. *Science* 2007;316:732.
- Liu LP, Zhuang ZB, Xie T, Wang YG, Li J, Peng Q, et al. *J Am Chem Soc* 2009;131:16423.
- Pillai V, Kumar P, Hou MJ, Ayyub P, Shah DO. *Adv Colloid Interface Sci* 1995;55:241.
- Pilemi MP. *Nat Mater* 2003;2:145.
- Eastoe J, Hollamby MJ, Hudson L. *Adv Colloid Interface Sci* 2006;128:5.
- Qi LM. Synthesis of inorganic nanostructures in reverse micelles. In: Somasundaran P, editor. *Encyclopedia of Surface and Colloid Science*. Second Edition. New York: Taylor & Francis; 2006. p. 6183.
- Bumajdad A, Eastoe J, Mathew A. *Adv Colloid Interface Sci* 2009;147–148:56.
- Ganguli AK, Ganguly A, Vaidya S. *Chem Soc Rev* 2010;39:474.
- Eastoe J, Warne B. *Curr Opin Colloid Interface Sci* 1996;1:800.
- Hegmann T, Qi H, Marx VM. *J Inorg Organomet Polym Mater* 2007;17:483.
- Gao Y, Hao JC. *J Phys Chem B* 2009;113:9461.
- Liu FL, Shen Q, Su YL, Han SH, Xu GY, Wang DJ. *J Phys Chem B* 2009;113:11362.
- Yang P, Lipowsky R, Dimova R. *Small* 2009;5:2033.
- Ma YR, Qi LM. *J Colloid Interface Sci* 2009;335:1.
- Lehn JM. *Angew Chem Int Ed Engl* 1988;27:89.
- He YF, Fu P, Shen XH, Gao HC. *Micron* 2008;39:495.
- Harada A, Hashidzume A, Yamaguchi H, Takashima Y. *Chem Rev* 2009;109:5974.
- Antonietti M, Kuang DB, Smarsly B, Yong Z. *Angew Chem Int Ed Engl* 2004;43:4988.
- Li ZG, Jia Z, Luan YX, Mu TC. *Curr Opin Solid State Mater Sci* 2008;12:1.
- Ma Z, Yu JH, Dai S. *Adv Mater* 2010;22:261.
- Dupont J. *J Braz Chem Soc* 2004;15:341.
- Leclercq L, Schmitzer A. *Supramol Chem* 2009;21:245.
- Binnemans K. *Chem Rev* 2005;105:4148.
- Henglein A. *J Phys Chem* 1993;97:5457.
- Hodak JH, Henglein A, Hartland GV. *J Phys Chem B* 2000;104:9954.
- Belloni J, Mostafavi M, Remita H, Marignier JL, Delcourt MO. *New J Chem* 1998;22:1239.
- Belloni J. *Catal Today* 2006;113:141.
- Buxton GV, Greenstock CL, Helman WP, Ross AB. *J Phys Chem Ref Data* 1988;17:513.
- Wardman P. *J Phys Chem Ref Data* 1989;18:1637.
- Zhu YJ, Qian YT, Cao YF. *Mater Sci Eng B-Solid State Mater Adv Technol* 1999;57:247.
- Zhu YJ, Qian YT, Hai H, Zhang MW. *J Mater Sci Lett* 1996;15:1700.
- Zhu YJ, Qian YT, Hai HA, Zhang MW. *Mater Lett* 1996;28:119.
- Zhu YJ, Qian Y. *Mater Sci Eng B-Solid State Mater Adv Technol* 1997;47:184.
- Hullavarad NV, Hullavarad SS, Karulkar PC. *J Nanosci Nanotechnol* 2008;8:3272.
- Ni YH, Ge XW, Xu XL, Chen JF, Zhang ZC. *J Inorg Mater* 2000;15:9.
- Chen QD, Bao HY, Shen XH. *Radiat Phys Chem* 2008;77:974.
- Bagwe RP, Khilar KC. *Langmuir* 1997;13:6432.
- Modes S, Lianos P. *J Phys Chem* 1989;93:5854.
- Qi LM, Ma JM, Cheng HM, Zhao ZG. *Colloid Surf A-Physicochem Eng Asp* 1996;108:117.
- Kitchens CL, McLeod MC, Roberts CB. *Langmuir* 2005;21:5166.
- Destree C, Nagy JB. *Adv Colloid Interface Sci* 2006;123:353.
- Spirin MG, Brichkin SB, Razlimov VF. *J Colloid Interface Sci* 2008;326:117.
- Ranjan R, Vaidya S, Thaplyal P, Qamar M, Ahmed J, Ganguli AK. *Langmuir* 2009;25:6469.
- Qi LM, Ma JM, Cheng HM, Zhao ZG. *J Phys Chem B* 1997;101:3460.
- Hopwood JD, Mann S. *Chem Mater* 1997;9:1819.
- Shi HT, Qi LM, Ma JM, Wu NZ. *Adv Funct Mater* 2005;15:442.
- Filankembo A, Giorgio S, Lisiecki I, Pilemi MP. *J Phys Chem B* 2003;107:7492.
- Kurihara K, Kizling J, Stenius P, Fendler JH. *J Am Chem Soc* 1983;105:2574.
- Wu HK, Xu XL, Ge XW, Zhang ZC. *Radiat Phys Chem* 1997;50:585.
- Egorova EM, Revina AA. *Colloid J* 2002;64:301.
- Kapoor S, Joshi R, Mukherjee T, Mittal JP. *Res Chem Intermed* 2001;27:747.
- Kapoor S, Joshi R, Mukherjee T. *Chem Phys Lett* 2004;396:415.
- Kapoor S, Adhikari S, Gopinathan C, Mittal JP. *Mater Res Bull* 1999;34:1333.
- Revina AA, Oksentyuk EV, Fenin AA. *Protect Met* 2007;43:554.
- Gornostaeva SV, Fenin AA, Revina AA, Ermakov VI. *Theor Found Chem Eng* 2008;42:599.
- Xu CQ, Ni YH, Zhang ZC, Ge XW, Ye Q. *Mater Lett* 2003;57:3070.
- Liu WJ, He WD, Zhang ZC, Zheng C, Li J, Jiang H, et al. *J Cryst Growth* 2006;290:592.
- Chen J, Wang X, Zhang Z. *Mater Lett* 2008;62:787.
- Xu CQ, Zhang ZC, Wang HL, Ye Q. *Mater Sci Eng B-Solid State Mater Adv Technol* 2003;104:5.
- Gotic M, Jurkin T, Music S. *Colloid Polym Sci* 2007;285:793.
- Gotic M, Jurkin T, Music S. *Mater Res Bull* 2009;44:2014.
- Wong M, Gratzel M, Thomas JK. *Chem Phys Lett* 1975;30:329.
- Gebicki JL, Gebicka L, Kroh J. *J Chem Soc-Faraday Trans* 1994;90:3411.
- Adhikari S, Joshi R, Gopinathan C. *J Colloid Interface Sci* 1997;191:1268.
- Adhikari S, Joshi R, Gopinathan C. *Int J Chem Kinet* 1998;30:699.
- Joshi R, Mukherjee T. *Radiat Phys Chem* 2003;66:397.
- Pilemi MP, Brochette P, Hickel B, Lerebours B. *J Colloid Interface Sci* 1984;98:549.
- Pilemi MP, Hickel B, Ferradini C, Pucheault J. *Chem Phys Lett* 1982;92:308.
- Calvoperez V, Beddard GS, Fendler JH. *J Phys Chem* 1981;85:2316.
- Chen QD, Shen XH, Gao HC. *J Colloid Interface Sci* 2007;308:491.
- Giorgi R, Bozzi C, Dei LG, Gabbiani C, Ninham BW, Baglioni P. *Langmuir* 2005;21:8495.
- He P, Shen XH, Gao HC. *J Colloid Interface Sci* 2005;284:510.
- Zhang X, Xie Y, Xu F, Liu X, Xu D. *Inorg Chem Commun* 2003;6:1390.
- Wang ZL, Feng XD. *J Phys Chem B* 2003;107:13563.
- Lu CH, Qi LM, Yang JH, Wang XY, Zhang DY, Xie JL, et al. *Adv Mater* 2005;17:2562.
- Ng CHB, Fan WY. *J Phys Chem B* 2006;110:20801.
- Xu HL, Wang WZ, Zhu W. *J Phys Chem B* 2006;110:13829.
- Jiao SH, Xu LF, Jiang K, Xu DS. *Adv Mater* 2006;18:1174.
- Kuo CH, Huang MH. *J Phys Chem C* 2008;112:18355.
- Liang XD, Gao L, Yang SW, Sun J. *Adv Mater* 2009;21:2068.
- Zhang DF, Zhang H, Guo L, Zheng K, Han XD, Zhang Z. *J Mater Chem* 2009;19:5220.
- Qi LM, Ma JM, Shen JL. *J Colloid Interface Sci* 1997;186:498.
- Chen QD, Shen XH, Gao HC. *J Colloid Interface Sci* 2007;312:272.
- Yang Z, Chiang CK, Chang HT. *Nanotechnology* 2008;19:7.
- Tang BX, Guo SM, Zhang MB, Li JH. *Synthesis* 2008;1707.
- Biswas K, Varghese N, Rao CNR. *Small* 2008;4:649.
- Kim BJ, Tersoff J, Kodambaka S, Reuter MC, Stach EA, Ross FM. *Science* 2008;322:1070.
- Rempel JY, Bawendi MG, Jensen KF. *J Am Chem Soc* 2009;131:4479.
- Mosseri S, Henglein A, Janata E. *J Phys Chem* 1989;93:6791.
- Ershov BC, Janata E, Henglein A. *Radiat Phys Chem* 1992;39:123.
- Ershov BC, Henglein A. *J Phys Chem* 1993;97:3434.
- Henglein A, Gutierrez M, Janata E, Ershov BC. *J Phys Chem* 1992;96:4598.
- Kelm M, Lilie J, Henglein A, Janata E. *J Phys Chem* 1974;78:882.
- Henglein A, Janata E, Fojtik A. *J Phys Chem* 1992;96:4734.
- Michaelis M, Henglein A. *J Phys Chem* 1992;96:4719.
- Zheng J, Petty JT, Dickson RM. *J Am Chem Soc* 2003;125:7780.
- Wilcoxon JP, Martin JE, Parsapour F, Wiedenman B, Kelley DF. *J Chem Phys* 1998;108:9137.
- He P, Shen XH, Gao HC. *Acta Phys-Chim Sin* 2004;20:1200.
- Liu J, Alvarez J, Kaifer AE. *Adv Mater* 2000;12:1381.
- Kim JH, Kim KS, Manesh KM, Santhosh P, Gopalan AL, Lee KP. *Colloid Surf A-Physicochem Eng Asp* 2008;313–314:612.
- Park C, Youn H, Kim H, Noh T, Kook YH, Oh ET, et al. *J Mater Chem* 2009;19:2310.
- Chen Y, Liu Y. *Chem Soc Rev* 2010;39:495.
- Denicourt-Nowicka A, Ponchel A, Monflier E, Roucoux A. *Dalton Trans* 2007:5714.
- Depalo N, Comparelli R, Striccoli M, Curri ML, Fini P, Giotta L, et al. *J Phys Chem B* 2006;110:17388.
- Xu JZ, Xu S, Geng J, Li GX, Zhu JJ. *Ultrason Sonochem* 2006;13:451.
- Li LD, Sun XH, Yang YL, Guan NJ, Zhang FX. *Chem Asian J* 2006;1:664.
- Sun XH, Zheng CM, Zhang FX, Li LD, Yang YL, Wu GJ, et al. *J Phys Chem C* 2008;112:17148.
- Cruz LAC, Perez CAM, Romero HAM, Casillas PEG. *J Alloy Compd* 2008;466:330.
- Kumar RV, Koltypin Y, Xu XN, Yeshurun Y, Gedanken A, Felner I. *J Appl Phys* 2001;89:6324.
- Liu LY, Male KB, Bouvrette P, Luong JHT. *Chem Mater* 2003;15:4172.
- Kabashin AV, Meunier M, Kingston C, Luong JHT. *J Phys Chem B* 2003;107:4527.
- Huang Y, Li D, Li JH. *Chem Phys Lett* 2004;389:14.



- [117] Huang T, Meng F, Qi LM. *J Phys Chem C* 2009;113:13636.
- [118] Liu J, Mendoza S, Roman E, Lynn MJ, Xu RL, Kaifer AE. *J Am Chem Soc* 1999;121:4304.
- [119] Liu J, Ong W, Roman E, Lynn MJ, Kaifer AE. *Langmuir* 2000;16:3000.
- [120] Liu Z, Jiang M. *J Mater Chem* 2007;17:4249.
- [121] Jing B, Chen X, Wang XD, Zhao YR, Qiu HY. *ChemPhysChem* 2008;9:249.
- [122] Ng CHB, Yang JX, Fan WY. *J Phys Chem C* 2008;112:4141.
- [123] Pande S, Ghosh SK, Praharaj S, Panigrahi S, Basu S, Jana S, et al. *J Phys Chem C* 2007;111:10806.
- [124] Nowicki A, Zhang Y, Leger B, Rolland JP, Bricout H, Monflier E, et al. *Chem Commun* 2006:296.
- [125] Komiyama M, Hirai H. *Bull Chem Soc Jpn* 1983;56:2833.
- [126] Willner I, Mandler D. *J Am Chem Soc* 1989;111:1330.
- [127] Messner M, Kurkov SV, Jansook P, Loftsson T. *Int J Pharm* 2010;387:199.
- [128] Edwards HE, Navaratnam S, Parsons BJ, Philips GO. *Radiation Biology and Chemistry*. New York: Elsevier; 1979.
- [129] Phillips GO, Young M. *J Chem Soc (A)* 1966:383.
- [130] Phillips GO, Young M. *J Chem Soc (A)* 1966:393.
- [131] Yang SG, Chen QD, Shi JF, Shen XH. *Acta Phys-Chim Sin* 2010;26:805.
- [132] Zhai ML, Yi M, Ha HF. *Radiation Process Technology and Development in Polymer Materials*. Beijing: Chemical Industry Press; 2004.
- [133] Lopes J, Padua AAH. *J Phys Chem B* 2006;110:3330.
- [134] Triolo A, Russina O, Bleif HJ, Di Cola E. *J Phys Chem B* 2007;111:4641.
- [135] Adhikari A, Sahu K, Dey S, Ghosh S, Mandal U, Bhattacharyya K. *J Phys Chem B* 2007;111:12809.
- [136] Grodkowski J, Neta P, Wishart JF. *J Phys Chem A* 2003;107:9794.
- [137] Wishart JF, Neta P. *J Phys Chem B* 2003;107:7261.
- [138] Wishart JF, Lall-Ramnarine SI, Raju R, Scumpia A, Bellevue S, Ragbir R, et al. *Radiat Phys Chem* 2005;72:99.
- [139] Shkrob IA, Wishart JF. *J Phys Chem B* 2009;113:5582.
- [140] Behar D, Gonzalez C, Neta P. *J Phys Chem A* 2001;105:7607.
- [141] Grodkowski J, Neta P. *J Phys Chem A* 2002;106:5468.
- [142] Imanishi A, Tamura M, Kuwabata S. *Chem Commun* 2009:1775.
- [143] Tsuda T, Seino S, Kuwabata S. *Chem Commun* 2009:6792.
- [144] Bosse E, Berthon L, Zorz N, Monget J, Berthon C, Bisel I, et al. *Dalton Trans* 2008:924.
- [145] Chen SM, Liu YD, Wu GZ. *Nanotechnology* 2005;16:2360.
- [146] Ghosh HN, Sapre AV, RamRao KVS. *Chem Phys Lett* 1996;255:49.
- [147] Qiu ZM, Texter J. *Curr Opin Colloid Interface Sci* 2008;13:252.
- [148] Hao JC, Zemb T. *Curr Opin Colloid Interface Sci* 2007;12:129.
- [149] Greaves TL, Drummond CJ. *Chem Soc Rev* 2008;37:1709.